

## Nonlinear dielectric response of glasses at low temperature

S. Rogge, D. Natelson, B. Tigner, and D. D. Osheroff

*Department of Physics, Stanford University, Stanford, California 94305-4060*

(Received 24 September 1996)

We have measured the dielectric response of amorphous insulators in the audio frequency range at temperatures between 500  $\mu$ K and 400 mK. We compare the measured superlinear behavior with a model incorporating higher order terms at low frequencies. Temperature independent dielectric response at low fields and low temperatures has also been observed which may indicate a low energy cutoff in the two-level system distribution of order 1 mK in some materials. We also find anomalously high sensitivity of the dielectric response to rf noise. [S0163-1829(97)09817-2]

### I. INTRODUCTION

In 1971 Zeller and Pohl<sup>1</sup> presented data showing the universal anomalous thermodynamic properties of noncrystalline materials at low temperatures. Instead of a Debye specific heat these systems are dominated by a semilinear term at low temperature,  $C \propto T^{1.2} + T^3$ . Anderson, Halperin, and Varma and independently Phillips<sup>2,3</sup> developed a model attributing the additional term in the heat capacity to the existence of defects due to the disorder which are not present in crystals. In the model the defects are represented by noninteracting two-level systems with a distribution of energy splittings and tunneling barriers. Assuming a flat distribution of energy splittings and tunneling parameters (flat in  $\lambda$  which defines the tunneling element  $\Delta = \hbar \Omega e^{-\lambda}$  where  $\Omega$  is the attempt frequency), the model predicts a specific heat that is linear in temperature and a  $T^2$  thermal conductivity, as is also observed.

In 1972 Jäckle<sup>4</sup> calculated the saturable acoustic absorption of the TLS which soon thereafter was experimentally verified in a glass. Knowing the absorption, one can find the nondissipative response by using the Kramers-Kronig relation. The same formalism holds for the dielectric response of the system. In these calculations linear response of the system must be assumed, since the Kramers-Kronig relation is strictly a linear response theory. Recently other authors<sup>5,6</sup> have used a different approach to calculate both the in and out of phase components of the response directly from the dynamics of the system, including nonlinear processes.

### II. THEORY: NONLINEAR RESPONSE

The low temperature acoustic and dielectric response of amorphous systems is described by the interaction of the TLS with the phonons and external fields. There are two limits for the response to an external field, the resonant and relaxational regimes. In the low temperature limit (resonant regime) TLS's are coherently driven by the external fields. At higher temperatures the system is dominated by one-phonon relaxations of the TLS up to roughly 1 K (relaxational regime), where multiphonon processes become important.

The acoustic and dielectric response of the glass is given by the integration of the single TLS response over the pa-

rameter distribution of the TLS (asymmetry energy  $\hbar \nu$  and tunneling parameter  $\Delta$ ),

$$\bar{\chi}(\omega) = \hbar \int_{\Delta_{\min}}^{\Delta_{\max}} \frac{d\Delta}{\Delta} \int_0^{\nu_{\max}} d\nu \chi(\Delta, \nu, \omega). \quad (1)$$

In the acoustic case the response manifests itself as a change in the speed of sound ( $\delta v$ ) and internal friction ( $Q^{-1}$ ), while in the dielectric case one observes changes in the capacitance ( $\delta \epsilon$ ) and loss factor ( $\tan \phi$ ). These quantities are given by

$$\delta v/v = -2C_a \text{Re} \bar{\chi}(\omega), \quad Q^{-1} = 4C_a \text{Im} \bar{\chi}(\omega), \quad (2)$$

$$\delta \epsilon/\epsilon = 2C_d \text{Re} \bar{\chi}(\omega), \quad \tan \phi = 4C_d \text{Im} \bar{\chi}(\omega), \quad (3)$$

with  $C_a = P \gamma^2 / \rho v^2$  and  $C_d = 2 P p^2 / 3 \epsilon_0 \epsilon$ . Here  $p = \langle |\vec{p}| \rangle$  is the average magnitude of the electric dipoles in the material,  $\epsilon$  the dielectric constant of the bulk,  $P$  the number of TLS's per unit volume per unit energy,  $\gamma$  the TLS phonon coupling constant,  $\rho$  the density of the material, and  $v$  the bulk speed of sound.

The paper by Stockburger *et al.*<sup>6</sup> is concerned with the acoustic response of an insulating reed at low frequency and temperature. We can compare our dielectric data to their model since both the acoustic and dielectric responses are based on the same mechanism. In the acoustic case all TLS's absorb phonons in a resonant or relaxational manner. In the dielectric case a subset of these TLS's with permanent electric dipoles<sup>7</sup> interact with an external electric field in the same fashion. The only difference is the number of TLS's that are active.

The authors of the paper<sup>6</sup> calculate the generalized susceptibility from a rate equation. For low temperature (resonant tunneling regime) they find superlinear behavior of the response which turns into a drive independent plateau at very low temperature. The temperature scale is defined by the crossover from the relaxational response (higher temperatures) to the resonant response (low temperature). This crossover is reflected by a maximum in the speed of sound and a minimum in the capacitive response. Below and above the temperature of the minimum the capacitance is predicted to depend logarithmically on temperature with a slope ratio of  $S_{\text{low}} : S_{\text{high}} = -2 : 1$ . The relaxational contribution does not depend on the drive level and so the minimum of  $\epsilon'(T)$  is shifted toward higher temperatures as the drive is increased,

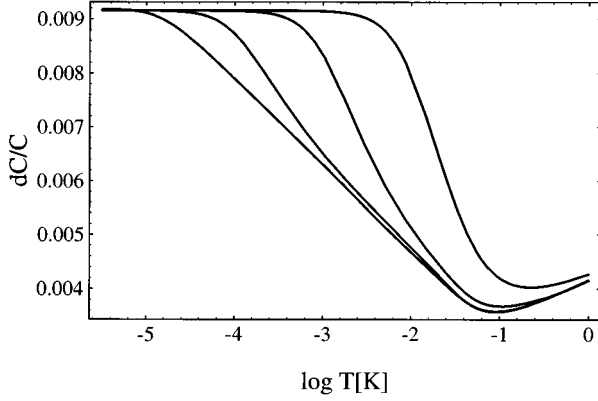


FIG. 1. This figure shows the superlinear behavior and saturation of the resonant contribution to the dielectric response calculated from the Stockburger model. All logarithms in the plots are base 10. The curves from bottom to top represent drive levels equivalent to 0.03, 0.3, 3, and 30 mK. The nonlinear behavior becomes dominant when  $\vec{p} \cdot \vec{E}_{ac}$  is comparable to  $kT$ . The curve for the strongest drive shows the steepest low temperature slope and reaches the temperature and drive independent plateau first. The value for the plateau is set by  $-C_d \ln(\hbar \Delta_{min}/2E_{max})$ . The low energy cutoff for the tunneling parameter was set to  $\hbar \Delta_{min}/k = 10^{-5}$  K, the high energy cutoff of the TLS spectrum is  $E_{max}/k = 10$  K, and the other material constants are chosen for BK7:  $\omega = 2\pi 500$  Hz,  $\gamma = 0.65$  eV,  $Pp^2 = 7.36 \times 10^{-14}$  C J $^{-1}$  m $^{-1}$ ,  $\epsilon_{bulk} = 7$ ,  $\rho = 2510$  kg m $^{-3}$ ,  $v = 4190$  ms $^{-1}$ . The calculation is based on an extrapolation of the tabulated integrals by Stockburger *et al.*

Fig. 1. The figure also shows the drive independent plateau of the capacitance at low temperature. The response becomes temperature and field independent when the low temperature cutoff in the tunneling parameter,  $\hbar \Delta_{min}/k$ , becomes comparable to the temperature. The response becomes superlinear when the energy associated with the driving field,  $pE_{ac}$ , where  $E_{ac}$  is the measuring field, becomes comparable to  $kT$ .

The standard parameters of the linear dielectric response model are the mentioned phonon coupling constant  $\gamma$ , an overall scale factor  $Pp^2$ , and the high energy cutoff  $E_{max}$ . In the nonlinear model two additional parameters are important for the dielectric response: the size of the drive (given by  $pE_{ac}$ ) and the low energy cutoff of the tunneling parameter  $\Delta_{min}$ . Figure 1 showed the effect of the drive with a constant low energy cutoff. Figure 2 demonstrates the effect of changing  $\Delta_{min}$  at constant drive. The parameter,  $\Delta_{min}$ , does not influence the temperature where the response becomes super-

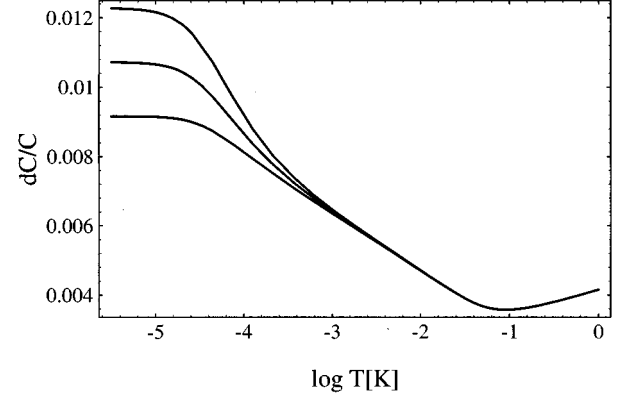


FIG. 2. This figure shows the saturation effect for three values of  $\Delta_{min}$  (top to bottom:  $\hbar \Delta_{min}/k = 10^{-7}$ ,  $10^{-6}$ , and  $10^{-5}$  K) at a constant drive of  $10^{-4}$  K. The onset temperature of nonlinearities does not change but their magnitude does, which leads to different plateau heights.

linear, but does determine the size of the nonlinearity (plateau height) and the temperature where the capacitance becomes independent of drive and temperature (low drive and low temperature limit).

### III. EXPERIMENTAL SETUP

Our audiofrequency capacitance measurements were done with a standard three-terminal bridge.<sup>8</sup> For the ultralow temperature data we used optical isolators to separate our analog bridge from the digital data acquisition. We found the samples to be extremely sensitive to high frequency noise, rf, which is discussed in detail in a separate section. Good rf shielding and heat sinking of the sample and leads was necessary to achieve the low temperature data presented. Our samples include a variety of thin glass films. The samples discussed in detail are the reactively sputtered  $3 \mu\text{m}$  thick  $\text{SiO}_x$ , both 5% and 10% potassium doped  $\text{SiO}_2$  glasses ( $\text{SiO}_2:\text{K}_2\text{O}$ ) which were ground down from bulk to  $20 \mu\text{m}$  BK7 (a standard optical glass) ground to  $50 \mu\text{m}$  thick, and a  $15 \mu\text{m}$  thick Mylar film (see Table I).

For the lowest temperatures discussed, we immersed the samples directly in  $^3\text{He}$  with two silver powder heat exchangers per electrode to heat sink the incoming leads and the sample electrodes to the  $^3\text{He}$  bath. The  $^3\text{He}$  was linked to the nuclear demagnetization stage by a silver powder heat exchanger ( $40 \text{ m}^2$ , similar to the one discussed in Ref. 9). Our thermometry consisted of a  $^3\text{He}$  melting curve thermometer, a paramagnetic salt susceptibility thermometer,

TABLE I. This table shows general properties of our samples.  $T_{sat}$  is the approximate temperature where the samples deviate from the predicted  $\log(T)$  behavior. The temperature of the minimum is given for 5 kHz and the low temperature slope is defined as  $S_T = \partial(\delta C/C)/\partial \log_{10}(T) \times 10^4$ .

| Sample                 | $T_{min}$ | $S_{temp}$ | $T_{sat}$   | Electrode | Thickness        |
|------------------------|-----------|------------|-------------|-----------|------------------|
| Mylar                  | 50 mK     | 3.5        | $\leq 1$ mK | CrAu      | 15 $\mu\text{m}$ |
| 5% K:SiO <sub>2</sub>  | 100 mK    | 8.6        | 4 mK        | CrAu      | 20 $\mu\text{m}$ |
| 10% K:SiO <sub>2</sub> | 100 mK    | 14.0       | 4 mK        | CrAu      | 20 $\mu\text{m}$ |
| BK7                    | 100 mK    | 22.0       | 5 mK        | CrAu      | 50 $\mu\text{m}$ |
| SiO <sub>x</sub>       | 80 mK     | 60.0       | 8 mK        | Nb        | 3 $\mu\text{m}$  |

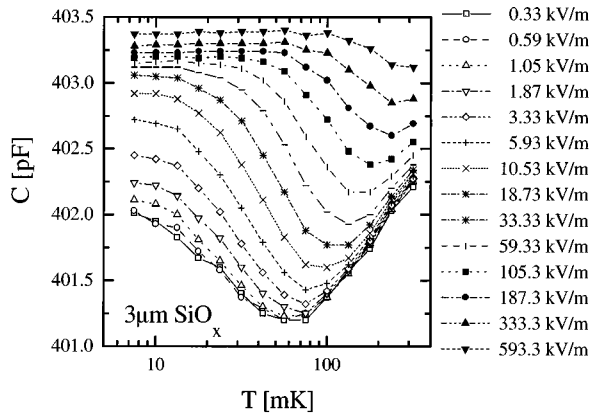


FIG. 3. This graph shows the capacitance at 2.2 kHz vs temperature for the 3  $\mu\text{m}$   $\text{SiO}_x$  sample mounted on sapphire in the top-load slug. The data show linear behavior in the field for small drive values. At high drive levels we see an enhanced low temperature response that shifts the minimum toward higher temperatures. There is also a low temperature saturation, but we have to neglect these data for this vacuum mount since the heat sinking of the sample is relatively poor.

and a  $^{195}\text{Pt}$  pulsed NMR thermometer immersed in the  $^3\text{He}$  bath. Each electrode of the glass sample had two heat exchangers which were thermally isolated from each other, and we were able to cool the samples to below 500  $\mu\text{K}$ . The high temperature data were taken with the samples mounted in a top-load configuration with faster response times. The  $^3\text{He}$  immersion cell has long thermal relaxation times above 100 mK due to the increasing heat capacity and decreasing thermal conductivity of the  $^3\text{He}$ .

#### IV. OBSERVATIONS

The observations are divided into three sections. First we will discuss the nonlinear behavior of our samples and compare it to the Stockburger model. Next and most importantly we will discuss the drive *independent* dielectric saturation at low temperature and low drive levels, and finally the extreme rf sensitivity of the dielectric response at low temperature.

##### A. Nonlinear dielectric response

Figure 3 shows the dielectric response of the  $\text{SiO}_x$  sample at various drive levels. The minimum in dielectric response is shifted toward higher temperatures as the drive is increased, which is the opposite of what one would expect from heating. The shift of the minimum results from the enhanced resonant contribution at low temperature. In this data run the sample is mounted in vacuum and the low temperature, high drive data have to be neglected due to heating concerns.

Including the  $\text{SiO}_x$  sample shown in Fig. 3 we always observed a slope ratio between the resonant and the relaxational regime which is different from the theoretically predicted  $-2:1$ . We consistently see a steeper rise of the relaxational contribution and find slope ratios in the linear regime between  $-2:1$  and  $-2:2$ . Other groups have also reported this discrepancy from the standard tunneling model, which

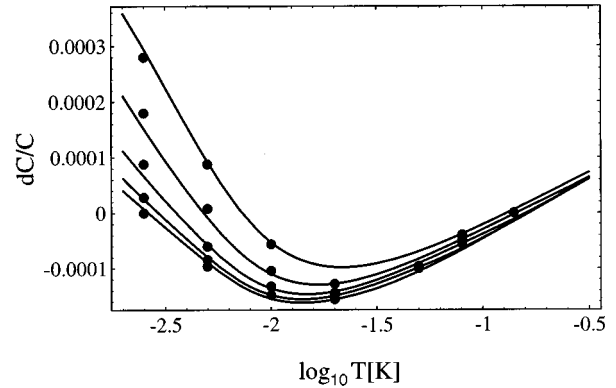


FIG. 4. The Stockburger *et al.* model does fit the Mylar data in this temperature range quite well, since we do not enter the saturation region. The data were taken at 5 kHz at driving fields of 1.25, 2.5, 5, 10, and 20 kV/m. This plot shows the fractional change in capacitance compared to the 140 mK point, subtracting a temperature independent but field dependent capacitive offset. The low field fit leads to a slope ratio of  $-2:1.1$ . The high field fit leads to a dipole moment of 1.9 Debye and a low energy cutoff  $\hbar \Delta_{\min}/k = 25 \mu\text{K}$ . Since we do not enter the saturation regime the values of these two parameters are just one of many possible pairs and so it is not surprising that the dipole moment is considerably larger than the one obtained by a nonequilibrium experiment with the same material ( $\approx 1$  D). All parameters are the same as for BK7 except for  $\rho = 1400 \text{ kg m}^{-3}$ ,  $v = 1.8 \text{ km s}^{-1}$ , and  $\epsilon_{\text{bulk}} = 4$ .

assumes that one-phonon processes dominate the system between the temperature of the minimum and 1 K.

The rest of the data discussed were all taken in the immersion cell, resulting in much better heat sinking. Figure 4 shows the dielectric response of the Mylar sample. The Mylar does not show dielectric saturation in the temperature regime accessible to us (down to 500  $\mu\text{K}$ ). The lines in the figure indicate a fit to the Stockburger model which is quite successful. This result was obtained by fitting the low field data with the linear response and then using these parameters to fit the nonlinear behavior, resulting in numbers for the dipole moment and the low energy cutoff of the tunneling parameter,  $\Delta_{\min}$ . Since we do not enter the plateau region we cannot determine the dipole moment and the low temperature cutoff independently (the parameters are discussed in the caption).

Figure 5 shows the attempted fit by the model to the BK7 data. The fit fails due to the qualitative difference between data and model. The data saturate in plateaus which are monotonically dependent on the measuring field while the model predicts one plateau (drive independent). The other discrepancy between the BK7 data and model is the onset temperature of the nonlinearities. In the models, the onset temperature is higher, but the nonlinearities are less steep.

In the plateau region we cannot completely rule out heating, due to the presence of the superlinear behavior. The superlinear behavior will cause an increased slope at low temperature which can then turn over into a plateau if the temperature of the sample is elevated above the temperature of the  $^3\text{He}$  (which we measure) due to dissipative heating by the driving field. The fact that we observe frequency dependence of the plateau at higher fields makes this argument plausible since dissipation is frequency dependent while the

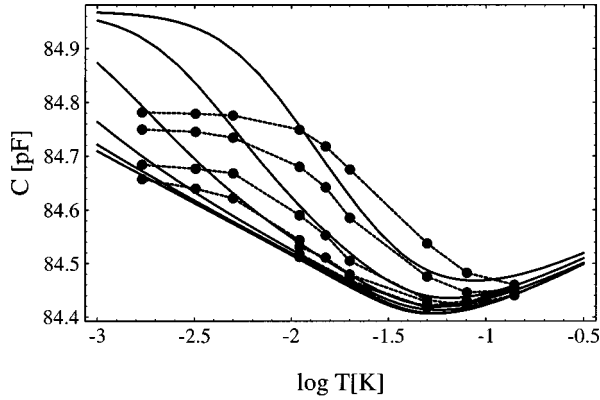


FIG. 5. This plot shows a least squares fit of the Stockburger *et al.* model to our BK7 immersion cell data at 500 Hz and fields of 0.2, 0.4, 1, 3, 9, and 24 kV/m. The low field fit resulted in a slope ratio of  $-2:1.4$  in contrast to the theoretically predicted ratio of  $-2:1$ . The high field fits yield a dipole moment of  $3.5 D$ , which is surprisingly large, and a low energy cutoff of  $\hbar\Delta_{\min}/k=50 \mu\text{K}$ , which is unreliable since the fit fails at high fields. Note the low temperature, high field limit: the data saturate in multiple plateaus in contrast to the Stockburger model.

capacitive response should be frequency independent. This would lead to a frequency dependent amount of heat dissipated in the sample, changing the point where the sample temperature began to differ from the  $^3\text{He}$  temperature.

We cannot rule out the heating model discussed in the last paragraph, but two other arguments have to be considered. As discussed below, we find a drive independent saturation for BK7 with a saturation temperature of 5 mK. If the low field plateau is not due to heating, the plateaus at higher capacitance due to higher drive cannot be explained by heating (see Fig. 1). Second, if we assume that the low field saturation is not due to intrinsic saturation but due to heating, we would expect a much bigger spread in the high field plateau capacitance in contrast to what we observe. To do a worst case analysis we consider the interface with the strongest temperature dependence between the sample and the  $^3\text{He}$  which is a phonon mismatch (proportional to  $T^3$ ). For the BK7, the ratio of the highest to lowest power input is greater than  $10^4$ , which would result in a saturation temperature increase of at least one decade. In this worst case scenario for the boundary resistance, we would expect the high field data to deviate from its logarithmic rise at a temperature at least a factor of 10 higher than for the low field data, which is not the case. Considering the two arguments presented we think the heating model plausible but not likely.

The Stockburger *et al.* model describes the data in the case of small nonlinearities and temperatures above the saturation temperature quite successfully (Mylar in Fig. 4 and also the potassium doped samples). We find discrepancies between our observations and the model at low temperatures and large drive levels. In contrast to the model we observe temperature independent but drive dependent regions at low temperature and large fields. The other discrepancy between the data and model is the fast onset of the nonlinearities at temperatures around the minimum at high fields (BK7 in Fig. 5 as well as the  $\text{SiO}_x$  sample). At low fields we observe drive

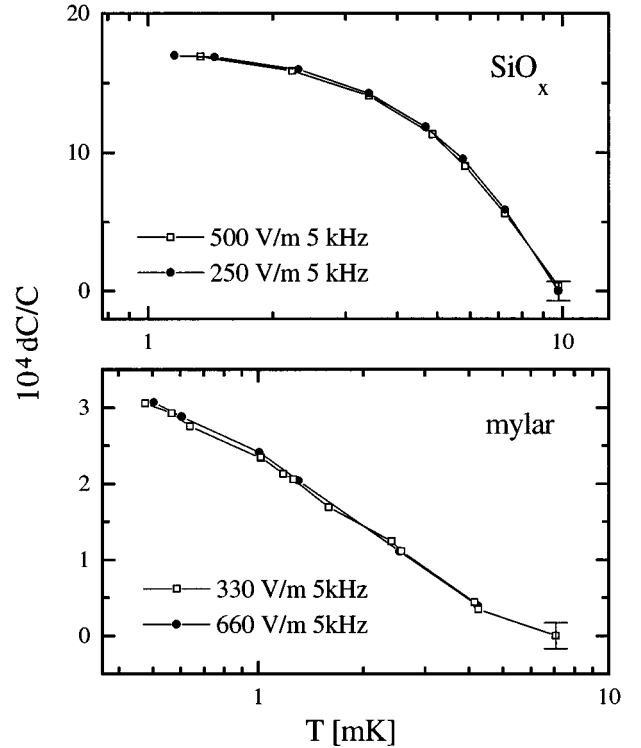


FIG. 6. These two plots show the drive independent low temperature behavior of the Mylar and  $\text{SiO}_x$  sample. The  $\text{SiO}_x$  clearly shows saturation while the Mylar stays logarithmic down to at least  $600 \mu\text{K}$ .

independent saturation which cannot be explained by heating. This limiting case of the model and the observations are described in the next section.

## B. Drive independent saturation

We now describe the low temperature saturation of the dielectric response at low drive levels; that is, the deviation from the  $\log(T)$  behavior leading into a temperature independent region. The temperature at which we observe significant deviation from the “ideal” behavior varies from material to material and Mylar does not show any saturation down to below  $500 \mu\text{K}$  (see Fig. 6). We also observe the drive independent saturation to be frequency independent.

We first address the question is saturation just due to heating of the sample above the temperature of the  $^3\text{He}$  which is measured by the Pt thermometer? We think we can rule this out. First, the observed behavior does not depend on the amplitude of the ac measuring field. For all the traces shown in Fig. 6 we have also used half the field across the sample and observed exactly the same behavior. For considerably higher fields there is frequency dependent saturation which is not field independent; as discussed above, this may be attributable to heating due to the higher loss of the sample at lower frequencies. Second, we observe the Mylar to obey  $\log(T)$  behavior down to below  $500 \mu\text{K}$  in the same environment where the other samples show saturation. All samples were heat sunk in the same fashion. We use two heat exchangers separated by a superconductor to ensure that no heat from the leads reaches the sample. We also checked for high frequency noise on our sample leads and injected addi-

TABLE II. This table shows the resulting  $\Delta_{\min}$  of the fit to the drive independent low field data, comparing it to the saturation temperature,  $T_{\text{sat}}$ , and the temperature slope,  $S_T = \partial(C/C_0)/\partial[\log_{10}(T)] \times 10^4$ . The energy associated with the ac drive field was conservatively estimated by using a dipole moment of one Debye. Note the monotonic dependence of the  $\Delta_{\min}$  parameter on the density of TLS's, which is proportional to  $S_T$ . The saturation temperature is higher than the expected onset of nonlinearities which occurs roughly at a temperature four times larger than the drive field, ruling out a heating effect.

| Sample                 | $S_{\text{temp}}$ | $T_{\text{sat}}$ | $\hbar\Delta_{\min}/k$ | $E_{\text{ac}}$ | Drive             |
|------------------------|-------------------|------------------|------------------------|-----------------|-------------------|
| Mylar                  | 3.5               | <1 mK            | $\leq 0.5$ mK          | 330 V/m         | 80 $\mu\text{K}$  |
| 5% K:SiO <sub>2</sub>  | 8.6               | 4 mK             | 1.3 mK                 | 500 V/m         | 120 $\mu\text{K}$ |
| 10% K:SiO <sub>2</sub> | 14.0              | 4 mK             | 1.4 mK                 | 250 V/m         | 60 $\mu\text{K}$  |
| BK7                    | 22.0              | 5 mK             | 2.2 mK                 | 200 V/m         | 50 $\mu\text{K}$  |
| SiO <sub>x</sub>       | 60.0              | 8 mK             | 3.3 mK                 | 250 V/m         | 60 $\mu\text{K}$  |

tional high frequency signals to quantify what rf levels are necessary to cause heating. For all samples except the SiO<sub>x</sub>, we conclude that the saturation is not due to heating from external heat sources like rf. The extreme sensitivity of the samples to high frequency noise is discussed in the next section.

We also ensured that we were in the linear response regime for these low field saturation measurements. The expected onset temperature for nonlinearities based on the Stockburger model for the fields used is much lower than the point at which we observe a departure from the ‘‘ideal’’ behavior, even with a conservative estimate of one Debye for the dipole moment of the sample; see Table II. This suggests that superlinear behavior did not enhance the response in the temperature independent region, which might have been lowered due to heating.

The low temperature saturation of the dielectric response may be explicable in the framework of the theory discussed above by  $\hbar\Delta_{\min}/k$  which is comparable to the saturation temperature. This means the density of states ends at this energy and lower temperatures will not reach any more TLS's; thus we observe a constant dielectric response. The parameter  $\hbar\Delta_{\min}$  refers to the largest tunneling barrier in the system ( $\Delta_{\min} = \Omega e^{-\lambda}$ , with  $\lambda \propto \sqrt{V}$  where  $V$  is the height of the barrier). In the low temperature, low field limit the TLS saturation capacitance is given by<sup>6</sup>

$$\frac{\epsilon_{\text{sat}}}{\epsilon} = C_d \ln \frac{\hbar\Delta_{\min}}{2E_{\text{max}}} + 1. \quad (4)$$

We obtain the values for the parameters  $\epsilon$ ,  $C_d$ , and  $E_{\text{max}}$  by fitting the linear response model to the unsaturated part of the curve. A fit like the one for SiO<sub>x</sub> shown in Fig. 7 leads to the quoted numbers of  $\Delta_{\min}$  in Table II. We find values for the low energy cutoff  $\hbar\Delta_{\min}/k$  from 3.3 mK for the SiO<sub>x</sub> to the Mylar sample where we do not observe any saturation in the low drive limit. It is reassuring to see a material dependence in this parameter, since the maximum barrier height should depend on the microscopic structure of the sample.

In ‘‘text book’’ calculations for the dielectric response  $\hbar\Delta_{\min}/k$  is often assumed to be on the order of  $10^{-8}$  to  $10^{-6}$  K. However, the interpretation of both recent heat pulse experiments<sup>10</sup> and heat capacity measurements by Lajunias *et al.*<sup>11</sup> by Strehlow *et al.*<sup>10,12</sup> find  $\hbar\Delta_{\min}/k$  to be on the order of 1 mK.

We note that the saturation temperature seems to be monotonic in the slope,  $S_T$  (Mylar to SiO<sub>x</sub>), which is interesting since there is no relation between the barrier height and  $Pp^2$  (which is proportional to  $S_T$ ) in the independent TLS model, nor in our understanding of glass formation. Another speculation for the low field saturation would be that interactions between the TLS create a cutoff in the TLS density of states at low energies. It is not trivial to describe this theoretically since one has to consider the collective motion of these clusters of TLS's which are expected to have smaller tunneling barriers. We note, however, that there should be no close relation between the strength of the interactions and  $S_T$ , since  $S_T$  depends only on that fraction of TLS's with dipole moments.

To study the importance of interactions on the density of states cutoff, one needs a set of samples with a controlled density of TLS's in the same host environment. If the interactions are dipole-dipole (electric) based, just the subsystem with electric dipole moments contributes. SiO<sub>2</sub> with different amounts of OH<sup>-</sup> doping would be a good candidate since it has been shown that the temperature slope varies linearly with the amount of OH<sup>-</sup> in the system.<sup>13</sup> For this system one

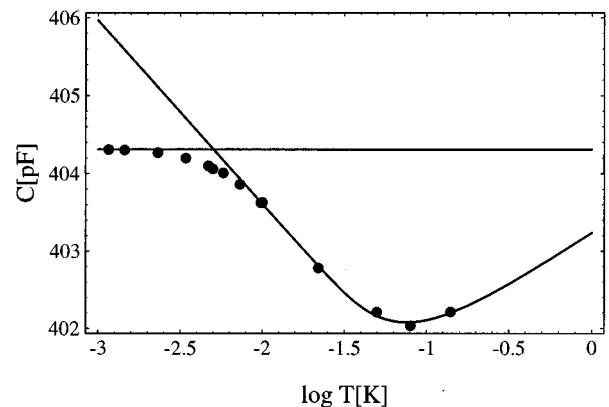


FIG. 7. This graph shows the low temperature saturation of SiO<sub>x</sub> with a driving field of 250 V/m at 5 kHz. The linear fit is based on temperatures above 10 mK excluding the saturation region. The line indicates the saturation value of the capacitance. In the case of drive independent saturation we can rule out the heating problem and the saturation capacitance can be translated into  $\Delta_{\min}$  by using the results of linear fit. This procedure leads to  $\hbar\Delta_{\min}/k = 3.3$  mK.

would expect to find a saturation monotonic in the  $\text{OH}^-$  density. However, if saturation occurs because all TLS's interact with each other, not just the ones with electric dipoles,  $\text{OH}^-$  doping of the  $\text{SiO}_2$  will only add to the small subset of TLS's. To study interactions in this case all TLS's have to be considered, including the ones without a permanent electric dipole moment.

We intended to test the importance of the electric dipolar interactions and performed the above experiment with doped samples by using  $\text{K}_2\text{O}$  in  $\text{SiO}_2$ ,<sup>14</sup> but could not come to a strong conclusion. Table II shows that the two doping levels (5 and 10 %) have almost the same value for  $\Delta_{\min}$ , although the low temperature slope of the two samples does not differ by a factor of 2 as expected from the doping level. We do not think that this effect is due to the TLS with electric dipoles that are not due to the  $\text{K}_2\text{O}$  doping, since the doping level is very high. This kind of composite glass is expected to form networks between the two components which does not lead to the isolated TLS sites that we need for this experiment.

It is interesting to note that the observed saturation temperatures and apparent  $\Delta_{\min}$  are not consistent with a model that links  $\Delta_{\min}$  with the glass transition.<sup>13</sup> The glass transition is defined by the viscosity of the glass, which can be modeled by a hopping process. The largest barriers in the system which define  $\Delta_{\min}$  should scale with  $T_g$ . This model would predict a small  $\Delta_{\min}$  for a system with a large  $T_g$  (i.e., large hopping barriers). This seems to be inconsistent with our observation that Mylar shows no saturation down to 500  $\mu\text{K}$ , since one expects a low  $T_g$  for a polymer leading to a large  $\Delta_{\min}$ . Furthermore, the  $\text{OH}^-$  content in  $\text{SiO}_2$  is not connected to the glass transition of  $\text{SiO}_2$ , but several groups have observed a strong dependence of the saturation temperature on the  $\text{OH}^-$  concentration. Nishiyama *et al.*<sup>15</sup> observed a saturation temperature of 3 mK in  $\text{SiO}_2$  with 1200 ppm  $\text{OH}^-$  in contrast to none down to 600  $\mu\text{K}$  at 1 ppm. They studied the saturation of the 1200 ppm sample quite extensively and showed that the saturation temperature was field and frequency independent.

Another problem associated with explaining the low temperature plateau by a high value of  $\Delta_{\min}$  is that nonequilibrium experiments in amorphous solids<sup>16,17</sup> have reported relaxations that last past  $10^5$  sec, indicating a maximum relaxation time which is considerably too large to be consistent with a  $\hbar\Delta_{\min}/k$  of 1 mK. Dielectric saturation is based on the lack of systems with an energy splitting of less than  $kT_{\text{sat}}$ . The energies of a TLS are given by  $E = \pm\hbar\sqrt{\Delta^2 + \nu^2}$ , and the low energy cutoff in  $\Delta$  proposed in the discussed model is based on the assumption of a flat distribution in the asymmetry  $\hbar\nu$  down to zero energy. If interactions create a low energy cutoff in the asymmetry (represented by a local strain field or electric field<sup>18,19</sup>), the low temperature saturation can be explained as a cutoff in  $\nu$  and is consistent with the long-term relaxations in these systems.

We observe the saturation temperature in the low drive limit to be monotonic in  $S_T$  for different materials. A noninteracting TLS analysis leads to large values of  $\hbar\Delta_{\min}$ , which is consistent with a recent interpretation of heat capacity measurements but seems inconsistent with long term relax-

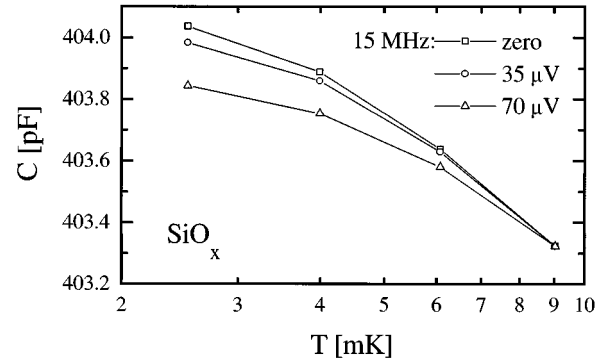


FIG. 8. This graph shows capacitance vs temperature data of the  $\text{SiO}_x$  sample at different rf levels. The top curve was obtained without an additional high frequency component, the lower ones at 35 and 70  $\mu\text{V}$  of the 15 MHz signal measured on top of the cryostat. The ac excitation used to measure the capacitance is 5 mV at 5 kHz. Note the appreciable effect due to 35  $\mu\text{V}$  rf compared to the existing audio drive of 5 mV.

ations observed in glasses. An interacting model, however, could also explain the saturation and would still be consistent with long relaxations.

### C. High frequency saturation-heating effects

During the measurements of the drive independent saturation at low drive levels we noticed that the capacitance of our samples was very sensitive to high frequencies. Figure 8 shows capacitance versus temperature for the  $\text{SiO}_x$  sample at low temperature with and without an additional rf field across the sample. Just 35  $\mu\text{V}$  at 15 MHz applied at the top of the cryostat alters the low temperature response at 5 kHz strongly. The power dissipated in the normal conducting leads of the sample and its electrodes is too small to explain this effect.

At  $T = 3$  mK the capacitance of the Mylar sample decreased the equivalent of a 1 mK temperature increase due to the application of 235  $\mu\text{V}_{\text{rms}}$  at 15 MHz with an audiodrive of 80  $\text{mV}_{\text{rms}}$  at 5 kHz, see Table III. The rf voltage is measured on top of the cryostat and to rule out resonance effects we changed the length of our coaxial cable outside the cryostat and saw no effect. One would not expect the glass to be more dissipative at higher frequencies since fewer TLS's can respond to the applied field. Yet, a rf field a factor of 1/300 or less in size of the audiodrive effects the dielectric response in the audio strongly.

Another possible explanation of the decrease in capacitance due to rf is the saturation of a portion of the TLS.<sup>20</sup> We repeated the experiment in the relaxational regime of the audio response ( $T > T_{\min}$  [5 kHz]) and applied 10 mV of rf across the leads of the Mylar sample at 40 mK. For the 15 MHz drive we are still well in the resonant regime at 40 mK. We observed an increase in capacitance, indicating a heating rather than saturation which would have caused a decrease in capacitance. If the effect is based on enhanced dissipation, it is not surprising that we had to use more voltage in this case, since the boundary resistance between the glass and the  $^3\text{He}$  drops for increasing temperature. We could not study this anomalous dissipation for high frequency quantitatively since in our setup we had no way of measuring the actual

TABLE III. The table shows the drop in capacitance due to the application of an additional field at 15 MHz across the 15  $\mu\text{m}$  thick Mylar sample. The change in capacitance was translated into an effective change in temperature. That drop in capacitance at temperatures below the temperature of the minimum and increase above indicate a heating effect. The temperature of the minimum in response of the Mylar is 23 mK at 1 kHz,  $S_T = \partial(C/C_0)/\partial[\log_{10}(T)] \times 10^4$ .

| $T$     | $S_T$ | $V_{\text{ex}}$ | $f_{\text{ex}}$ | $V_{15 \text{ MHz}}$ | $\delta C/C$          | $\delta T$ |
|---------|-------|-----------------|-----------------|----------------------|-----------------------|------------|
| 3.0 mK  | 5.40  | 80 mV           | 5 kHz           | 235 $\mu\text{V}$    | $-7.2 \times 10^{-5}$ | 1.0 mK     |
| 3.0 mK  | 5.40  | 80 mV           | 5 kHz           | 470 $\mu\text{V}$    | $-1.1 \times 10^{-4}$ | 1.8 mK     |
| 6.5 mK  | 5.40  | 80 mV           | 5 kHz           | 235 $\mu\text{V}$    | $-1.6 \times 10^{-5}$ | 0.5 mK     |
| 6.5 mK  | 5.40  | 80 mV           | 5 kHz           | 470 $\mu\text{V}$    | $-3.0 \times 10^{-5}$ | 1.0 mK     |
| 40.0 mK | 2.12  | 40 mV           | 1 kHz           | 10 mV                | $+1.9 \times 10^{-5}$ | 9.0 mK     |

voltage across the sample. All we have is an upper bound. Our studies suggest that the samples are more dissipative at high frequencies than expected from the standard TLS model, and it would be interesting to quantify this discrepancy.

## V. CONCLUSION

We have observed a superlinear resonant contribution to the dielectric response at low temperature as well as saturation behavior. Extreme rf sensitivity of the dielectric response was also observed, which is inconsistent with the expectation of a lower loss at higher frequencies. The main result of our measurements is the drive independent saturation at low fields. Using a noninteracting model to analyze our data leads to low energy cutoff in  $\Delta_{\text{min}}$  around 1 mK, which is consistent with a recent analysis of heat capacity

and heat pulse data resulting in a cutoff between 0.1 and 1 mK but inconsistent with long time relaxations observed in glasses. We suggest that a low energy cutoff in the asymmetry energy due to interactions could also explain the observations and still be consistent with long-term relaxations.

## ACKNOWLEDGMENTS

The authors wish to acknowledge useful discussions of their data and the theoretical background with Jürgen Stockburger. We also thank J.S. for granting us access to the tabulated functions based on his numerical work. D.N. wishes to acknowledge support from the Fannie and John Hertz Foundation. This work was supported under U.S. Department of Energy Grant Nos. DE-FG03-90ER45435 and DE-FG05-89ER75517.

<sup>1</sup>R. Zeller and R. Pohl, Phys. Rev. B **4**, 2029 (1971).

<sup>2</sup>P. Anderson, B. Halperin, and C. Varma, Philos. Mag. **25**, 1 (1972).

<sup>3</sup>W. Phillips, J. Low Temp. Phys. **7**, 351 (1972).

<sup>4</sup>J. Jäckle, Z. Phys. **257**, 212 (1972).

<sup>5</sup>D. Parshin, Z. Phys. B **91**, 367 (1993).

<sup>6</sup>J. T. Stockburger, M. Grifoni, and M. Sassetti, Phys. Rev. B **51**, 2835 (1995).

<sup>7</sup>C. Laermans, W. Arnold, and S. Hunklinger, J. Phys. C **10**, L161 (1977).

<sup>8</sup>B. Kibble and G. Rayner, *Coaxial AC Bridges* (Hilger, Bristol, 1984).

<sup>9</sup>R. C. Richardson and E. N. Smith, *Experimental Techniques in Condensed Matter Physics at Low Temperatures* (Addison-Wesley, Reading, MA, 1988).

<sup>10</sup>P. Strehlow and W. Dreyer, Physica B **194-196**, 485 (1994).

<sup>11</sup>J. Lasjaunias, R. Maynard, and M. Vandorpe, J. Phys. **39**, 973 (1978).

<sup>12</sup>M. Meissner and P. Strehlow, Czech. J. Phys. **46**, 2233 (1996).

<sup>13</sup>P. Strehlow (private communication).

<sup>14</sup>W. MacDonald, A. Anderson, and J. Schroeder, Phys. Rev. B **31**, 1090 (1985).

<sup>15</sup>H. Nishiyama, H. Akimoto, Y. Okuda, and H. Ishimoto, J. Low Temp. Phys. **89**, 727 (1992).

<sup>16</sup>D. Salvino, S. Rogge, B. Tigner, and D. Osheroff, Phys. Rev. Lett. **73**, 268 (1994).

<sup>17</sup>S. Rogge, D. Natelson, and D. Osheroff, Phys. Rev. Lett. **76**, 3136 (1996).

<sup>18</sup>S. Coppersmith, Phys. Rev. Lett. **67**, 2315 (1991).

<sup>19</sup>A. Burin, J. Low Temp. Phys. **100**, 309 (1995).

<sup>20</sup>C. Yu (private communication).